

Article

Improved Golden Jackal Optimization for Optimal Allocation and Scheduling of Wind Turbine and Electric Vehicles Parking Lots in Electrical Distribution Network Using Rosenbrock's Direct Rotation Strategy

Jing Yang ¹, Jiale Xiong ¹, Yen-Lin Chen ^{2,*}, Por Lip Yee ^{1,*}, Chin Soon Ku ^{3,*} and Manoochehr Babanezhad ⁴

- ¹ Department of Computer System and Technology, Faculty of Computer Science and Information Technology, Universiti Malaya, Kuala Lumpur 50603, Malaysia
² Department of Computer Science and Information Engineering, National Taipei University of Technology, Taipei 106344, Taiwan
³ Department of Computer Science, Universiti Tunku Abdul Rahman, Kampar 31900, Malaysia
⁴ Department of Statistics, Faculty of Sciences, Golestan University, Gorgan 49138-15759, Golestan, Iran
* Correspondence: ylchen@mail.ntut.edu.tw (Y.-L.C.); porlip@um.edu.my (P.L.Y.); kucs@utar.edu.my (C.S.K.)

Abstract: In this paper, a multi-objective allocation and scheduling of wind turbines and electric vehicle parking lots are performed in an IEEE 33-bus radial distribution network to reach the minimum annual costs of power loss, purchased grid energy, wind energy, PHEV energy, battery degradation cost, and network voltage deviations. Decision variables, such as the site and size of wind turbines and electric parking lots in the distribution system, are found using an improved golden jackal optimization (IGJO) algorithm based on Rosenbrock's direct rotational (RDR) strategy. The results showed that the IGJO finds the optimal solution with a lower convergence tolerance and a better (lower) objective function value compared to conventional GJO, the artificial electric field algorithm (AEFA), particle swarm optimization (PSO), and manta ray foraging optimization (MRFO) methods. The results showed that using the proposed method based on the IGJO, the energy loss cost, grid energy cost, and network voltage deviations were reduced by 29.76%, 65.86%, and 18.63%, respectively, compared to the base network. Moreover, the statistical analysis results proved their superiority compared to the conventional GJO, AEFA, PSO, and MRFO algorithms. Moreover, considering vehicles battery degradation costs, the losses cost, grid energy cost, and network voltage deviations have been reduced by 3.28%, 1.07%, and 4.32%, respectively, compared to the case without battery degradation costs. In addition, the results showed that the decrease in electric vehicle availability causes increasing losses for grid energy costs and weakens the network voltage profile, and vice versa.



Citation: Yang, J.; Xiong, J.; Chen, Y.-L.; Yee, P.L.; Ku, C.S.; Babanezhad, M. Improved Golden Jackal Optimization for Optimal Allocation and Scheduling of Wind Turbine and Electric Vehicles Parking Lots in Electrical Distribution Network Using Rosenbrock's Direct Rotation Strategy. *Mathematics* **2023**, *11*, 1415. <https://doi.org/10.3390/math11061415>

Academic Editors: Aspassia Daskalopulu and Dimitrios Bargiolas

Received: 14 February 2023

Revised: 9 March 2023

Accepted: 13 March 2023

Published: 15 March 2023



Copyright: © 2023 by the authors. Licensee MDPI, Basel, Switzerland. This article is an open access article distributed under the terms and conditions of the Creative Commons Attribution (CC BY) license (<https://creativecommons.org/licenses/by/4.0/>).

1. Introduction

Progress and the development of sustainable energy can be realized with proper preservation and maintenance of the environment. For this reason, clean emission-free power generation units are in demand for the upcoming years. Industry relies on energy and what has fueled international concerns in the field of energy are the limited resources of fossil fuels [1]. Electricity production via renewable energy is among the acceptable solutions to save nature and the environment. One of the energy sources of interest is wind energy [2]. Simple and cheap to access as well as the minimal environmental impacts of wind energy sources, which are one of the cleanest sources of energy, have caused

the designers of power networks to pay special attention to this source of energy [2]. That being said, however, the transportation sector is also looking to substitute internal combustion cars with electric vehicles (EVs) [3]. Due to the limited capacity of electric vehicles, they cannot affect the power network alone. Therefore, in this situation, electric parking lots have been provided to affect the characteristics of the network by placing several electric vehicles in them and by providing the ability to connect to the power network (V2G) [3,4]. Distribution networks are the final link in the electric energy supply chain for consumers. Therefore, the economic and technical efficiency of these networks as much as possible guarantees a stable and reliable future in the electricity industry. In this regard, it will be very important to examine the role of electric parking [3,4]. For the greater effectiveness of electric vehicles as well as renewable energy sources in distribution networks and management of vehicle charging and discharging, various objectives are proposed, including reducing costs, reducing power losses, and improving the voltage profile in distribution networks [3,4]. On the other hand, the allocation of wind energy resources and electric parking lots in the distribution network without technical scheduling and optimal sizing leads to economic problems for the parking investor and technical problems for the operator of the distribution network [4,5]. To overcome the non-linear nature of the problems related to the placement and sizing of wind energy sources as well as the electric parking lots in the distribution network, the use of meta-heuristic algorithms is considered [6,7]. Therefore, using a powerful optimization algorithm to solve the problem can be very useful.

In the following, some important studies relating to EV parking lots in the distribution network have been reviewed. In [8], the optimal siting of multiple energy resources based on HOMER software is discussed to design parking lots with the aim of minimizing the lifetime cost and the pollutant emissions. In [9], a multi-objective method is presented to allocate electric parking lots in the distribution system using a genetic algorithm (GA) to reduce power losses and increase the profitability of these types of parking lots. In [10], the combined tabu search—greedy random adaptive search—is presented for locating and optimizing the size of electric parking lots and their charging patterns with the aim of minimizing the operating cost. In [11], determining the optimal location and size of electric parking lots in the distribution system is developed to minimize power loss and improve the energy supply capability of subscribers. In [12], the location and optimal size of electric parking lots in the distribution system have been determined by evaluating the economic indices and the interaction between the owner of the parking lot and the operator of the distribution system. In [13], the scheduling of electrical parking lots in the distribution network in India is developed to reduce power loss using a hybrid GA-PSO algorithm. In [14], optimal planning of a hybrid energy system, including electric parking and photovoltaic energy sources, has been implemented using the BAT algorithm to minimize network costs. In [15], the optimal allocation of photovoltaic energy resources along with electric parking lots in the radial distribution system is presented to deal with power loss based on an optimization algorithm named technique for order preference by similarity to an ideal solution (TOPSIS). In [16], the optimal allocation of electric parking lots in the distribution network to decrease power loss and voltage variations of the network buses is presented by adopting GA and PSO algorithms. In [17], the optimal energy management of electric parking is developed by determining the optimal charging and discharging schedule of EVs while considering the energy cost. In [18], the scheduling of EV parking lots is presented with the aim of increasing the profitability of the parking lot owner. In [19], the optimal allocation of EV parking lots for charging electric vehicles to maximize energy costs is developed based on the fuzzy PSO. In [20], the optimal planning of electric parking lots in the power network has been investigated to maximize the income and decrease power loss, as well as deal with voltage deviations. In [21], optimal siting and sizing of electric parking lots in the radial distribution network are discussed using the combined harmony search-learning algorithm.

According to the literature review, it can be seen that most of the studies conducted to determine the optimal place and scale of energy sources, where optimal energy scheduling of parking lots is concerned, are based on meta-heuristic algorithms, and many of these methods have complex structures and adjustable control parameters. There are many adjustments, which is one of the challenges of these solvers to reach early and local optimal convergence. On the other hand, some studies have presented a complex mathematical structure of the system model as well as a meta-heuristic method that requires a large amount of data. Compared to analytical algorithms, meta-heuristic algorithms have easier implementation, fewer control parameters, and a higher response speed [22,23]. Additionally, the interaction effect of integrated wind energy with electric vehicle parking scheduling, considering the availability of EVs, on the cost imposed by power loss, the cost due to purchasing network power, and the voltage profile of the electrical network has not been well addressed. Therefore, based on the investigations, it is necessary to provide an improved meta-heuristic framework with effective optimization power against premature convergence conditions for the multi-objective placement and scheduling of wind energy sources and EV parking lots in the electricity distribution system.

The present research focuses on the multi-objective siting and scheduling of wind turbines and electric parking lots in the 33-bus distribution system to minimize the cost imposed by energy loss, main grid energy cost, wind energy cost, PHEVs' energy cost, and battery degradation cost, in addition to improving the network voltage profile using an improved meta-heuristic algorithm. The wind turbine is installed in such a way that, in interaction with the parking lots, it achieves the best value of each of the objectives presented in the problem's objective function. The decision variables include the optimal placement and scaling of wind turbines and PHEVs in the distribution system, which are optimally found by adopting a novel metaheuristic algorithm called the improved golden jackal optimization (IGJO) algorithm. The common golden jackal optimization (GJO) algorithm is an algorithm based on biological swarm intelligence that is presented based on the hunting behavior of golden jackals. The traditional GJO [24] suffers from issues in the form of imbalance between exploration and exploitation as well as getting caught in premature convergence. In this study, to improve the performance of the traditional GJO against these problems, Rosenbrock's direct rotational (RDR) method [25,26] is used. A comparison is conducted between the performance of the IGJO when applied to solve the problem and that of the commonly used GJO, PSO, AEFA, and MRFO. Moreover, due to the importance of vehicle availability in parking lots, their effectiveness in solving the problem and each of the objectives has been examined.

The contributions of the paper are presented below:

- Multi-objective allocation and scheduling of wind energy and electric parking lots at the distribution level to find the optimal installation point and size of the equipment, considering battery degradation cost.
- Providing a multi-objective function, including the minimization of energy loss costs, main grid energy costs, wind energy costs, and PHEV energy costs, in addition to improving the network voltage profile.
- Evaluating the impact of vehicle availability on problem solving and the objectives of energy losses, main grid energy cost, and network voltage profile.
- Providing an improved golden jackal optimization algorithm based on Rosenbrock's direct rotation strategy by creating a balance between the exploration and exploitation phases and effective performance in the case of premature convergence.
- Superiority of the proposed improved meta-heuristic method over GJO, AEFA, PSO, and MRFO in problem solving.

Section 2 describes the objective function of the problem and its constraints during the optimization process. Section 3 presents the proposed improved meta-heuristic method of golden jackal optimization based on Rosenbrock's direct rotation and explains how it works. In Section 4, a simulation report using different meta-heuristic algorithms and the

evaluation of the effect of EV availability in parking lots are presented. In Section 5, the findings of the paper are concluded and future work is suggested.

2. Problem Formulation

2.1. Objective Function

The allocation and scheduling of wind turbines and EV parking lots is a multi-objective optimization problem to minimize the costs of power loss, energy purchased from the main grid, wind power, charging and discharging PHEV energy, battery degradation, and bus minimization voltage variations. The formulation is stated as follows:

$$F^{OF} = \varphi_1 \times \left(C_{Loss}^{OF} / C_{Loss,max}^{OF} \right) + \varphi_2 \times \left(C_{Grid}^{OF} / C_{Grid,max}^{OF} \right) + \varphi_3 \times \left(C_{WT}^{OF} / C_{WT,max}^{OF} \right) \\ + \varphi_4 \times \left(C_{PHEVs}^{OF} / C_{PHEVs,max}^{OF} \right) + \varphi_5 \times \left(V_{VD}^{OF} / V_{VD,max}^{OF} \right) + \varphi_6 \times \left(C_{Deg}^{OF} / C_{Deg,max}^{OF} \right) \quad (1)$$

where, C_{Loss}^{OF} , C_{Grid}^{OF} , C_{WT}^{OF} , C_{PHEVs}^{OF} , V_{VD}^{OF} , and C_{Deg}^{OF} refer to the energy loss cost, grid energy cost, wind energy cost, PHEVs' energy cost, network bus voltage deviations, and battery degradation cost, respectively. $C_{Loss,max}^{OF}$, $C_{Grid,max}^{OF}$, $C_{WT,max}^{OF}$, $C_{PHEVs,max}^{OF}$, $V_{VD,max}^{OF}$, and $C_{Deg,max}^{OF}$, respectively, represent the upper limits of energy loss cost, grid energy cost, wind energy cost budget, PHEV energy cost budget, network bus voltage deviations, and the maximum cost of battery degradation. φ_1 , φ_2 , φ_3 , φ_4 , φ_5 and φ_6 , respectively, refer to the weight of inertia of the objective functions is the costs of power loss, network energy, wind energy, PHEV energy, the voltage deviations of the buses, and battery degradation cost, and the relationship $|\varphi_1 + \varphi_2 + \varphi_3 + \varphi_4 + \varphi_5 + \varphi_6| = 1$ is established.

By implementing the power flow of the basic network (without using electric parking lots and renewable energy sources), the values of power losses cost, the cost of power purchased from the main network, as well as the total amount of voltage deviations of the network buses are obtained, which represent the maximum values of the cost of power losses, the cost of power purchased from the main network, and total voltage deviations. Additionally, the maximum cost of electric parking lots and wind energy sources is considered the maximum budget for these costs. Based on the maximum capacity selected for parking lots and wind energy resources, naturally, the maximum budget for the cost of electric parking lots and also the cost of wind power has been determined. After determining the maximum values of each part of the general objective function, Equation (1) has been normalized using the method of weighted coefficients. Considering the number of five objectives and the total value of the weight coefficients, which should be equal to 1, the weight of each objective is considered 0.2.

- Cost of energy losses

The network power loss can be defined as the product of power loss on the network lines at the cost of each kW loss for the simulation period as follows [27–30].

$$C_{Loss}^{OF} = C_{Loss} \cdot \sum_{h=1}^H \sum_{i=1}^{N_{branch}} R_i \times |I_i(h)|^2 \quad (2)$$

C_{Loss} shows the cost per kW of power losses, N_{branch} is the number of distribution network lines, R_i is the ohmic resistance of line i , $I_i(h)$ denotes the current of line i at time h , and H is the duration of the simulation period (8760 h).

- Cost of main grid energy

The cost due to energy purchased from the main grid is calculated based on the product of the power received from the network and the cost of each kW of network power as follows [22,23].

$$C_{Grid}^{OF} = C_{Grid} \cdot \sum_{h=1}^H E_{Grid}(h) \quad (3)$$

where C_{Grid} and $E_{Grid}(h)$ represent the price of each kW of network power and the energy received from the network at time h , respectively.

- Cost of wind energy

In the following, the cost related to wind turbine power is modeled. This power is based on the output power of the turbine (taking into account the cut-in, cut-out, and rated wind speed, as well as the rated power of the turbine), and the cost per kW of wind turbine output power is formulated below [31–33].

$$C_{WT}^{OF} = C_{WT} \cdot \sum_{h=1}^H P_{WT}(h) \quad (4)$$

$$P_{WT}(h) = \begin{cases} 0 & ; v < v_{ci}, v > v_{co} \\ P_{WT-Nominal} \times \left(\frac{v(h)-v_{ci}}{v_r-v_{ci}} \right) & ; v_{ci} \leq v < v_r \\ P_{WT-Nominal} & ; v_r \leq v \leq v_{co} \end{cases} \quad (5)$$

where C_{WT} represents the cost per kW of wind power and P_{WT} shows the power generated by wind turbines. v_{ci} , v_{co} , and v_r are the cut-in, cut-out, and rated wind speeds, respectively. $P_{WT-Nominal}$ represents the rated power of the wind turbine.

- Cost of PHEVs cost

The energy cost of PHEVs (C_{PHEVs}^{OF}) is defined as below based on the charging and discharging energy of electric parking lots [22,23].

$$C_{PHEVs}^{OF} = C_{PHEVs} \cdot \sum_{h=1}^H P_{PHEVs}(h) \quad (6)$$

$$P_{PHEVs}(h) = P_{Discharge}(h) - P_{Charge}(h) \quad (7)$$

where C_{PHEVs} is the cost per kWh of PHEVs energy, $P_{PHEVs}(h)$ refers to the PHEVs power at time h , and $P_{Charge}(h)$ and $P_{Discharge}(h)$ are the charge and discharge energy of PHEVs, respectively.

- Voltage deviations of the network

Another objective considered is the minimization of network bus voltage deviations, which is defined as follows [34]:

$$V_{VD}^{OF} = \sqrt{\frac{1}{N_{bus}} \times \sum_{i=1}^{N_{bus}} (v_i - v_p)^2} \quad (8)$$

$$v_p = \frac{1}{N_{bus}} \times \sum_{i=1}^{N_{bus}} v_i \quad (9)$$

where N_{bus} is the number of distribution network buses, v_i is the voltage of bus i , and v_p is the reference voltage (1 p.u.).

- Cost of vehicles battery degradation cost

The battery degradation cost is presented by [35]

$$C_{Deg,max}^{OF} = \frac{C_{inv} \times DOD \times SOC_{PHEVs} \times \Delta h}{N_{CL}} \quad (10)$$

where C_{inv} represents the investment cost of the battery, Δh is the time interval (1 h). The depth of discharge (DOD) of the battery pack is calculated as follows [35]:

$$DOD = \frac{SOC_{PHEVs,max} - SOC_{PHEVs}}{SOC_{PHEVs,max}} \quad (11)$$

The cycle life of the battery can be expressed by Equation (11):

$$N_{CL} = \chi \times DOD^\sigma \quad (12)$$

where χ and σ represent the specific parameters of the battery, which are 1331 and –1.825 [35] for lithium ion batteries, respectively.

2.2. Constraints

The objective function defined in the multi-objective placement and scheduling of wind turbines and electric parking lots in the distribution network must satisfy the following constraint [22,23,27–30].

- Power balance

$$\sum_{h=1}^H P_{WT}(h) + \sum_{h=1}^H P_{Grid}(h) + \sum_{h=1}^H P_{PHEVs}(h) - \sum_{h=1}^H P_{Loss}(h) - \sum_{h=1}^H P_{Load}(h) = 0 \quad (13)$$

$$\sum_{h=1}^H Q_{WT}(h) + \sum_{h=1}^H Q_{Grid}(h) + \sum_{h=1}^H Q_{PHEVs}(h) - \sum_{h=1}^H Q_{Loss}(h) - \sum_{h=1}^H Q_{Load}(h) = 0 \quad (14)$$

where $P_{WT}(h)$ and $Q_{WT}(h)$ show the active and reactive power output of the wind turbine, $P_{Grid}(h)$ and $Q_{Grid}(h)$ express the active and reactive power received from the network, $P_{PHEVs}(h)$ and $Q_{PHEVs}(h)$ are the active and reactive power of PHEVs, $P_{Loss}(h)$ and $Q_{Loss}(h)$ refer to the active and reactive losses of the network at time h , and $P_{Load}(h)$ and $Q_{Load}(h)$ are the active and reactive load demand of the network at time h .

- Voltage constraint

The bus voltages during problem solving should not exceed the allowed range [27–31].

$$V_{\min}^{Network} \leq V^{Network} \leq V_{\max}^{Network}, \quad V = [V_1 \ V_2 \ \dots \ V_{N_{bus}}] \quad (15)$$

where, $V_{\min}^{Network}$ and $V_{\max}^{Network}$ are the lower and upper limit values of the voltage, respectively, and V refers to the vector of network bus voltage.

- Flow of lines

The current value of each of the network lines during problem solving should not exceed its allowed range [27–31].

$$I_{\min}^{Line} \leq I^{Line} \leq I_{\max}^{Line}, \quad I = [I_1 \ I_2 \ \dots \ I_{N_{branch}}] \quad (16)$$

where I_{\min}^{Line} and I_{\max}^{Line} are the lower and upper limit values of voltage, respectively, and I refers to the vector of network line current.

- Battery capacity of PHEVs

The state of charge (SOC) of the PHEVs battery units at any time h must obey the following inequality:

$$SOC_{PHEVs,min} \leq SOC_{PHEVs}(h) \leq SOC_{PHEVs,max} \quad (17)$$

where $SOC_{PHEVs,min}$ and $SOC_{PHEVs,max}$ are the lower and upper limits of the battery bank SOC, respectively.

The SOC_{PHEVs} value is defined as follows [22,23]:

$$SOC_{PHEVs}(h) = SOC_{PHEVs}(h - 1) + P_{charge}(h) \cdot \xi(h) - P_{discharge}(h) \cdot \tau(h) \quad (18)$$

$$\xi(h) + \tau(h) \leq 1 \quad (19)$$

$$\xi(h) = \begin{cases} 1, & \text{charge state of batteries} \\ 0 & \text{discharge state of batteries} \end{cases} \quad (20)$$

$$\tau(h) = \begin{cases} 1, & \text{discharge state of batteries} \\ 0 & \text{charge state of batteries} \end{cases} \quad (21)$$

where, $SOC_{PHEVs}(h)$ and $SOC_{PHEVs}(h - 1)$ are the battery SOC at time h and $h - 1$, respectively. $\xi(h)$ and $\tau(h)$ have different values at different hours based on the charging and discharging states of the battery (0 or 1), which are included in Equation (18).

3. Proposed Optimization Method

3.1. Golden Jackal Optimization (GJO)

GJO imitates biological swarm intelligence, which is modeled according to the hunting behavior of golden jackals. The hunt relies on three phases: (a) discovering the prey, (b) besieging and stimulating, and (c) attacking the prey [24]. In the following, the mathematical model of the GJO algorithm is formulated.

3.1.1. Search Model

During the first phase, the random position of the prey is defined as the following matrix [24]:

$$\begin{bmatrix} Y_{1,1} & Y_{1,j} & \cdots & \cdots & Y_{1,n} \\ Y_{2,1} & Y_{2,j} & \cdots & \cdots & Y_{2,n} \\ \vdots & \vdots & \vdots & \vdots & \vdots \\ \vdots & \vdots & \vdots & \vdots & \vdots \\ Y_{N,1} & Y_{N,j} & \cdots & \cdots & Y_{N,n} \end{bmatrix} \quad (22)$$

where N represents the number of prey populations and n refers to the dimensions.

3.1.2. Exploration Stage

Due to the inherent ability of jackals to follow the prey, it is not easy to catch the prey. Therefore, the jackals will be waiting to catch another prey. The hunting behavior can be defined by the following equations ($|E| > 1$) [24]:

$$Y_1(t) = Y_M(t) - E \cdot |Y_M(t) - rl \cdot Prey(t)| \quad (23)$$

$$Y_2(t) = Y_{FM}(t) - E \cdot |Y_{FM}(t) - rl \cdot Prey(t)| \quad (24)$$

t represents the current iteration of the algorithm, $Y_M(t)$ and $Y_{FM}(t)$ represent the locations of the male and female jackals, $Prey(t)$ represents the hunting position vector, and $Y_1(t)$ and $Y_2(t)$ determine the locations of jackals, of course, in an updated form.

The escape energy of prey (E) will be calculated by [24]:

$$E = E_1 \cdot E_0, \quad E_0 = 2 \cdot r - 1 \quad (25)$$

$$E_1 = c_1 \cdot \left(1 - \frac{t}{T}\right) \quad (26)$$

where E_0 represents a random number between -1 and 1 , T refers to the maximum number of iterations, c_1 represents a fixed number with a value of 1.5 , and E_1 refers to the reduction in the prey's energy [24].

In Equations (20) and (21), $|Y_M(t) - rl \cdot Prey(t)|$ refers to the distance between the jackal and the prey and "rl" represents the vector of random numbers determined based on the Le'vy flight function (LF) [24]:

$$rl = \frac{5 \cdot LF(y)}{100} \quad (27)$$

$$LF(y) = \frac{\mu \cdot \sigma}{100 \cdot \left| v^{\left(\frac{1}{\beta}\right)} \right|}, \quad \sigma = \left\{ \frac{\Gamma(1 + \beta) \cdot \sin(\frac{\pi \beta}{2})}{\Gamma(\frac{1+\beta}{2}) \cdot \beta \cdot (2^{\beta-1})} \right\}^{\frac{1}{\beta}} \quad (28)$$

where v represents values in the interval $(0, 1)$ randomly and β represents a fixed number with a considered value of 1.5 [24].

$$Y(t+1) = \frac{Y_1(t) + Y_2(t)}{2} \quad (29)$$

$Y(t+1)$ represents the updated location of the prey relative to jackals.

3.1.3. Exploitation (Besieging and Swallowing Prey)

The escape energy of prey is reduced by harassment by golden jackals. The behavior of jackals when besieging their prey and swallowing it can be modeled here ($|E| \leq 1$) [24]:

$$Y_1(t) = Y_M(t) - E \cdot |rl \cdot Y_M(t) - Prey(t)| \quad (30)$$

$$Y_2(t) = Y_{FM}(t) - E \cdot |rl \cdot Y_{FM}(t) - Prey(t)| \quad (31)$$

3.1.4. Transition from Exploration Stage to Exploitation and Convergence

In the GJO algorithm, it is used to transfer the exploration phase to exploiting the volatile energy of the prey. As the prey escapes, its energy decreases drastically. With this in mind, the escape energy of prey is modeled. The initial energy E_0 is indiscriminately deviated between -1 and 1 in each iteration. Once it decreases from 0 to -1 , it means that the prey is in danger, and if it increases from 0 to 1 , that means the prey's ability is enhanced. The escape energy of prey decreases with increasing repetitions. When $|E| > 1$, pairs of jackals explore different parts of the search space to discover prey. When $|E| < 1$, attacking the prey forms the exploitation stage. In the GJO, the search starts by considering a population of selected solutions. As the algorithm continues, the prey's location is estimated using a pair of jackals. Each candidate's response updates its position relative to the jackal pair. By reducing E_1 from 1.5 to 0 , exploration and exploitation stages are provided. In condition $E > 1$, the pair of jackals deviate from the prey, and in condition $E < 1$, they reach the prey. Finally, upon meeting the convergence conditions, the GJO algorithm stops.

The GJO pseudo-code is shown in Algorithm 1.

Algorithm 1. Pseudo-code of the GJO

Inputs: The population size N and maximum number of iterations T
Outputs: Prey's position and its fitness value
Set the random prey population Y_i ($i = 1, 2, \dots, N$)
While ($t < T$)
 Calculate the fitness values of prey
 Y_1 = best prey individual (location of the male jackal)
 Y_2 = second best prey individual (location of the female jackal)
 for (each of the preys)
 Update the escaping energy “ E ” based on (4) and (6)
 Update “ rl ” based on (6) and (7)
 If ($|E| \leq 1$) (Exploration phase)
 Update the prey's location based on (2), (3), and (8)
 If ($|E| > 1$) (Exploitation phase)
 Update the prey's location based on (8), (9), and (10)
 end for
 $t = t + 1$
end while
return Y_1

3.2. Overview of Improved GJO (IGJO)

The traditional GJO algorithm has problems in the form of imbalance between exploration and exploitation, as well as getting caught in premature convergence. In this article, to improve the performance of the traditional GJO algorithm against these problems, Rosenbrock's direct rotational (RDR) method [25,26] is used.

In the present case, the current phase is finished and the identification basis is checked to calculate the overall effect of successful phases in each of the dimensions [29]. The orthonormal basis has been updated as follows [25,26]:

$$x^{k+1} - x^{k+} = \sum_{i=1}^n \lambda_i \cdot d_i \quad (32)$$

In the equation below, a set of instructions is provided. λ_i represents the number of successful variables and $x^{k+1} - x^{k+}$ represents the point with the most useful search direction. Therefore, it is placed in the corrected search direction [25,26].

$$p_i = \begin{cases} d_i, & \lambda_i = 0 \\ \sum_{j=0}^n \lambda_j \cdot d_j & \lambda_i \neq 0 \end{cases} \quad (33)$$

Next, the search results based on the Gram–Schmidt normalization process are updated as the following equation [25,26].

$$q_i = \begin{cases} p_i, & i = 1 \\ p_i - \sum_{j=1}^{i-1} \frac{q_j^T \cdot p_i}{q_j^T \cdot q_j} & i \geq 2 \end{cases} \quad (34)$$

The modified and normalized search guidelines are defined as follows [25,26].

$$d_i = \frac{q_i}{\|q_i\|}, \quad i = 1, 2, 3, \dots, n. \quad (35)$$

After updating the local search, this method performs the search operation until the convergence condition of the algorithm is met in the new opposite direction.

3.3. Implementation of the IGJO

Figure 1 illustrates the flowchart of IGJO implementation in solving the problem. The procedures for siting and scheduling wind turbines and electric parking lots according to the IGJO approach in the distribution system are also presented below.

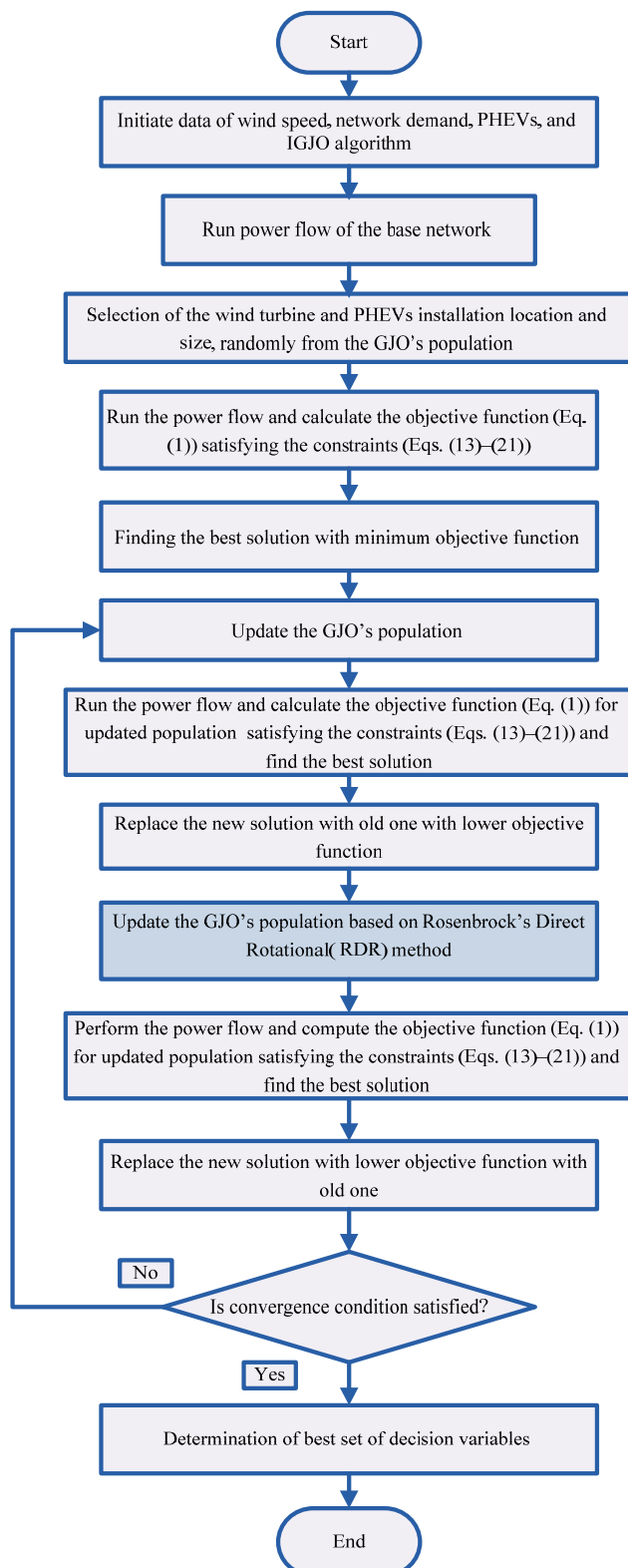


Figure 1. Flowchart of IGJO implementation to solve the problem.

Step 1. Application of distribution system data such as wind speed data, electric parking lots, network lines, and algorithm data including population, iteration, and repetition.

Step 2. Implementation of network load flow for the base network for a short term of 24 h and calculation of energy loss cost, grid energy cost, and network bus voltage deviations.

Step 3. The initial population of golden jackals is created randomly in the GJO algorithm. Each golden jackal randomly chooses several decision variables within the allowed boundary of the search space. The vector of decision variables includes the locations and capacities of wind turbines and electric parking lots.

Step 4. The load flow is performed and the objective function values (Equation (1)) are calculated considering the limitations of the problem (Equations (13)–(21)) for the set of variables selected in step 3. The variable set that leads to the minimized objective function will be the optimal solution.

Step 5. The population of golden jackals in the algorithm is updated by GJO and new variables are randomly chosen for the population.

Step 6. The load flow is performed and the objective function (Equation (1)) is computed for the new variables of step 5 by satisfying the constraints of the problem (Equations (13)–(21)). The variable set that minimizes the objective function will be the optimal solution at this stage and if the objective function value becomes lower than the previous solution, it is replaced with it.

Step 7. The population of the algorithm is updated based on Rosenbrock's direct rotation, and by applying the load flow, the value of the objective function (Equation (1)) is found for new random variables. Provided that the new solution is better, it replaces the one obtained in step 6.

Step 8. The convergence condition of the optimization algorithm is checked. If the minimum value of the objective function is reached, the algorithm goes to step 9, but if it isn't, it goes to step 3.

Step 9. The algorithm is stopped and the set of optimal variables is saved.

4. Simulation Results and Discussion

4.1. The Studied System

The proposed methodology based on IGJO was tested on a 33-bus distribution system. The schematic of this distribution network is depicted in Figure 2. The active and reactive power demands of the network are 3.72 MW and 2.3 MVar, respectively. The percentage of network peak load during 24 h is shown in Figure 3. In this study, a wind turbine with a peak capacity of 3000 kW is used, and the changes in wind speed during 24 h are shown in Figure 4. The technical and economic data of the equipment are listed in Table 1. In this study, the number of eight electric parking lots with a maximum capacity of five hundred vehicles is considered, and the optimization program determines how many parking lots and how many vehicles to install in the network. The battery capacity of each electric vehicle is 5 kWh, the V2G dispatch time is 3570 h per year, the penalty fee for each kWh of energy loss is \$0.06, and the cost of purchasing each kWh of main grid energy is \$0.1. In this study, the backward-forward power flow method is used to analyze the network characteristics. In this study, the performance of the IGJO algorithm in finding a solution to the problem of multi-objective siting and scheduling of wind turbines and EV parking lots in the distribution system has been compared with the traditional methods of GJO, AEFA, PSO, and MRFO. The control variables for different algorithms are given in Table 2. Note that the control parameters of the traditional GJO, AEFA, PSO, and MRFO methods are the values provided by their authors in reference papers. Based on the authors' experience, the population, maximum iteration, and independent executions of each algorithm are 50, 200, and 25, respectively.

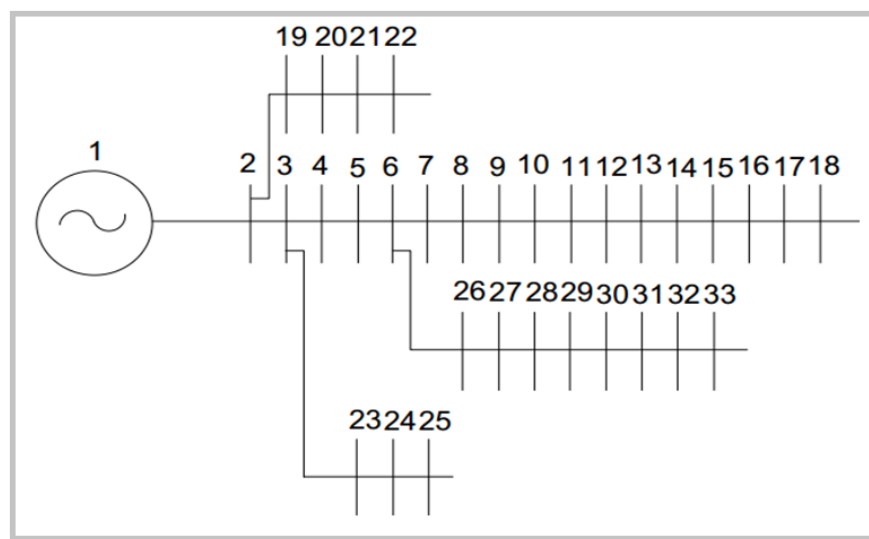


Figure 2. 33-base distribution network schematic.

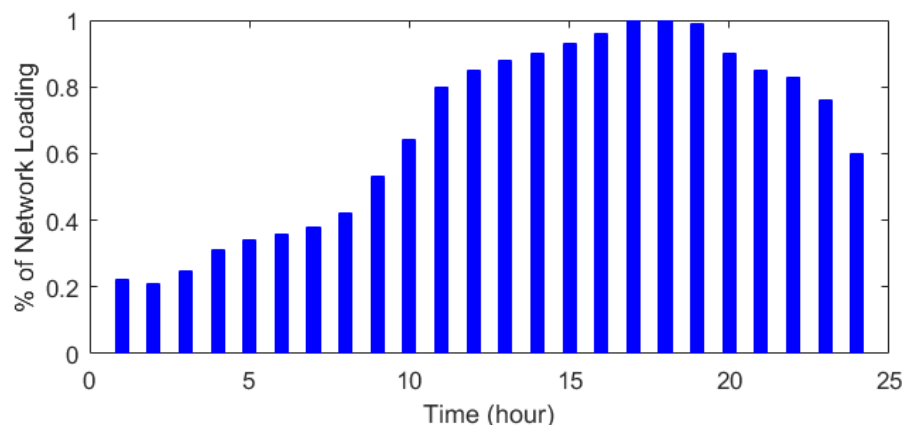


Figure 3. Network peak load percentage curve during 24 h.

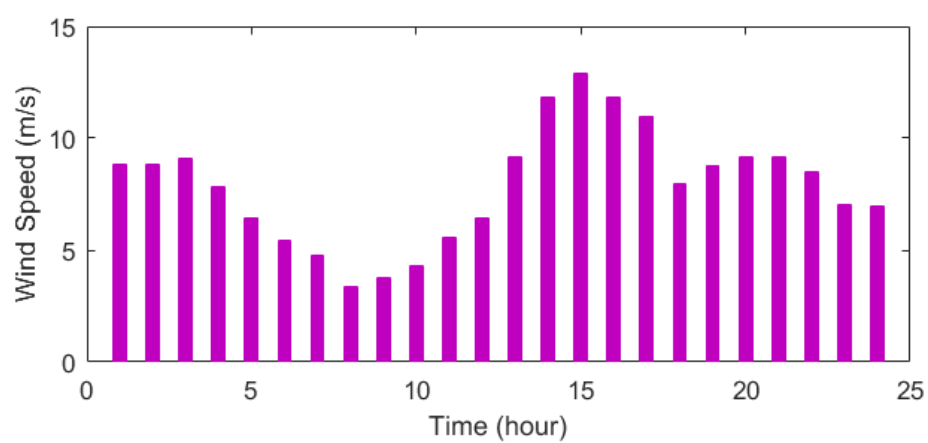


Figure 4. Changes in wind speed for 24 h.

Table 1. Technical-economic data on wind turbines, electric parking, and network.

Parameters	Values
C_{Loss} (\$/kWh)	0.06
C_{Grid} (\$/kWh)	0.1
C_{WT} (\$/kWh)	0.15
C_{PHEV} (\$/kWh)	0.1
v_{ci} (m/s)	3
v_r (m/s)	13
v_{co} (m/s)	20
$V_{min}^{Network}$ (p.u.)	0.95
$V_{max}^{Network}$ (p.u.)	1.05
$SOC_{PHEVs,min}$ (kWh)	1
$SOC_{PHEVs,max}$ (kWh)	5 kWh

Table 2. Control parameters for different algorithms.

Algorithm	Parameter	Value
AEFA	K0	500
	α	30
GJO	c1	1.5
	β	1.5
	C1	2
	C2	2
PSO	Inertia weight	Linearly reduction from 0.9 to 0.1
MRFO	S	2

4.2. Results without Battery Degradation Cost

Simulation results relating to the multi-objective allocation and scheduling of wind turbines and electric parking lots in the distribution system are provided to minimize energy loss costs, main grid energy costs, wind energy costs, and PHEV energy costs, in addition to improving the network voltage profile. Figure 5 illustrates the convergence curve of various algorithms used to solve the problem. According to Figure 5, the IGJO algorithm is able to achieve a lower objective function value with a lower convergence tolerance. It can be seen that the conventional GJO is trapped in the local optimum and could not converge to a lower objective function value such as the IGJO method. Therefore, the IGJO has obtained the optimal solution in comparison with the GJO, AEFA, PSO, and MRFO algorithms, in which the value of the objective function is the lowest. The most preferred (optimal) solution obtained by different algorithms in terms of siting and sizing of wind turbines and electric parking lots in the 33-bus distribution system is presented in Table 3. The IGJO installed 2941 kW of wind power in bus 6 and considered the number of five electric parking spaces in buses 7, 14, 21, 24, and 29 with the numbers of 80, 404, 41, 96, and 47 electric vehicles, respectively. Table 4 lists the numerical results of solving the problem. The values of the objective function obtained by the traditional GJO, AEFA, PSO, MRFO, and the proposed IGJO are 0.62739, 0.62979, 0.62722, 0.62679, and 0.62577, respectively, and the proposed improved algorithm obtains a lower (better) value. In addition, based on the results of the statistical analysis shown in Table 5, the IGJO algorithm has been confirmed to achieve the best index values during 25 independent executions of each algorithm. Based on the results of Table 4, compared to other methods, the IGJO achieved lower amounts of energy loss cost and main grid energy cost and also obtained lower voltage deviations, which indicates a further enhancement in the voltage profile. The power loss cost, network energy cost, and voltage deviations by IGJO are obtained at USD 37,596, USD 1,530,300, and 0.0140 p.u., respectively, and the percentage reduction in each objective is higher compared to other methods. Therefore, the proposed methodology has reduced the costs imposed by power loss, energy purchased from the power system, and voltage variations

in the 33-bus system compared to the basic state of the network by 29.76%, 65.86%, and 18.80%, respectively.

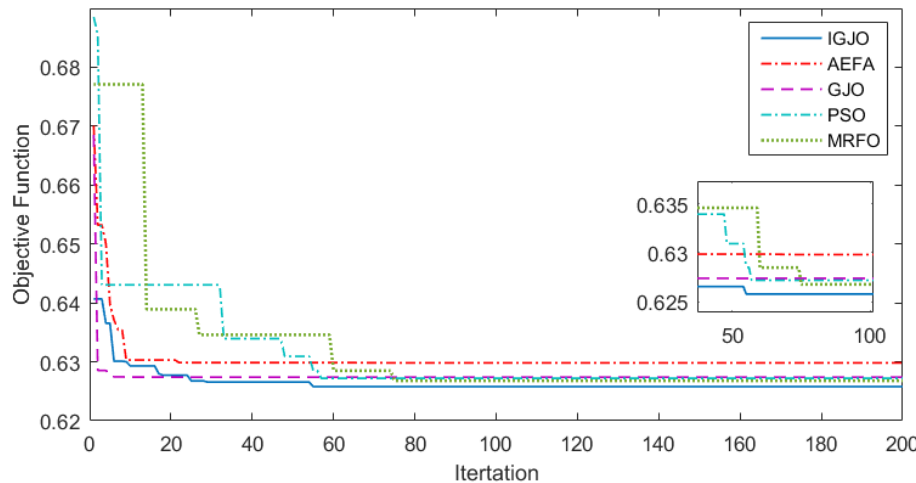


Figure 5. The convergence process of different algorithms in the allocation and scheduling of WT and PHEVs in the distribution network.

Table 3. The optimal solution using different algorithms.

Item/Algorithm	IGJO	AEFA	GJO	PSO	MRFO
WT Location @Bus/Peak size (kW)	@6/2941	@6/2454	@8/2996	@6/2354	@8/1913
PHEV Location @Bus/Size	@7/80, @14/404, @21/41, @24/96, @29/47	@8/369, @8/200, @21/200, @24/405 @29/266	@7/116, @8/200, @21/200, @25/138,	@14/500, @21/500	@7/243, @29/272, @31/342, @32/361

Table 4. The results of WT and PHEV scheduling in the distribution network using different algorithms.

Item/Algorithm	Base Network	IGJO	AEFA	GJO	PSO	MRFO
Cost of energy losses (\$)	53,531	37,596	43,200	37,740	37,714	37,696
Reduction in C_{Eloss} (%)	–	29.76	19.29	29.50	29.55	29.58
Cost of grid energy (\$)	4,482,550	1,530,300	1,855,297	1,566,600	1,561,680	1,553,800
Reduction in C_{Egrid} (%)	–	65.86	58.61	65.05	65.16	65.33
Voltage deviation (p.u.)	0.0173	0.0140	0.0154	0.0141	0.0141	0.0141
Reduction in VD (%)	–	18.80	10.58	18.63	18.63	18.63
Cost of PHEVs (\$)	–	620,356	819,491	824,610	841,017	885,450
Cost of WT (\$)	–	959,070	800,301	977,362	767,358	623,874
OF	–	0.62577	0.62979	0.62739	0.62722	0.62679

Table 5. The results of a statistic analysis of different algorithms.

Item/Algorithm	IGJO	AEFA	GJO	PSO	MRFO
Best	0.62577	0.62979	0.62739	0.62722	0.62679
Worst	0.62654	0.63254	0.62964	0.62851	0.62702
Mean	0.62615	0.63152	0.62873	0.62784	0.62696
Std	0.02212	0.04837	0.04652	0.03628	0.03845

The power variation curve of the wind turbine, with a peak power of 2941 kW obtained by the IGJO, is shown in Figure 6. Based on the best solution presented in Table 1, the power

loss, the power purchased from the upstream grid, and the minimum voltage changes in the 33-bus network during 24 h, as well as the network voltage profile curve, are presented in Figures 7–10. According to Figure 7, network power losses with the optimal and multi-objective scheduling of wind turbines and electric parking lots based on the IGJO, especially during the peak hours of the network between 12:00 and 22:00, compared to the basic state of the network, are significantly reduced (down 29.76%). Based on Figure 8, the power purchase from the power system has also decreased (65.86 percent decrease) when wind energy and EV parking lots operate optimally compared to without this equipments. Based on Figures 9 and 10, it can be seen that the optimal and multi-objective scheduling of wind energy and electric parking lots in the network has a positive effect on the network voltage and has improved the voltage profile of the 33-base network (18.80% improvement). The results show the reduction in the dependence of the distribution network based on optimal and multi-objective allocation and scheduling of wind energy and electric parking lots on the upstream grid.

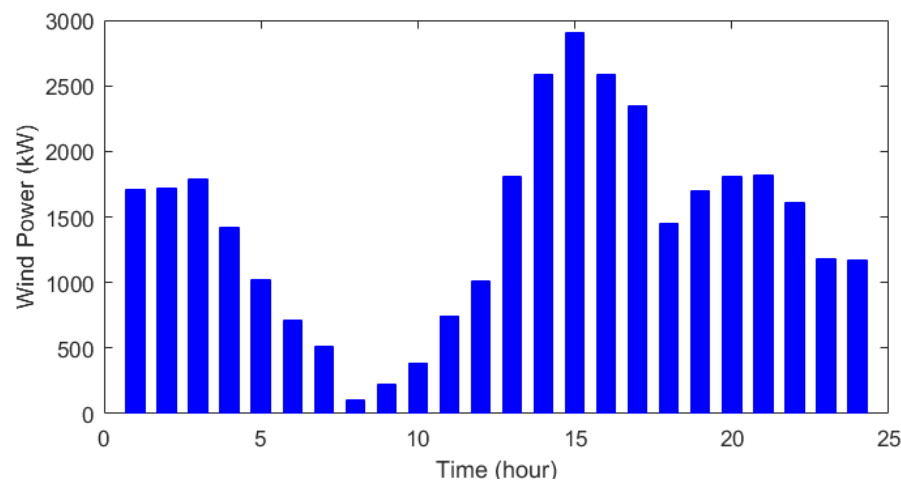


Figure 6. Wind power using the IGJO for 24 h.

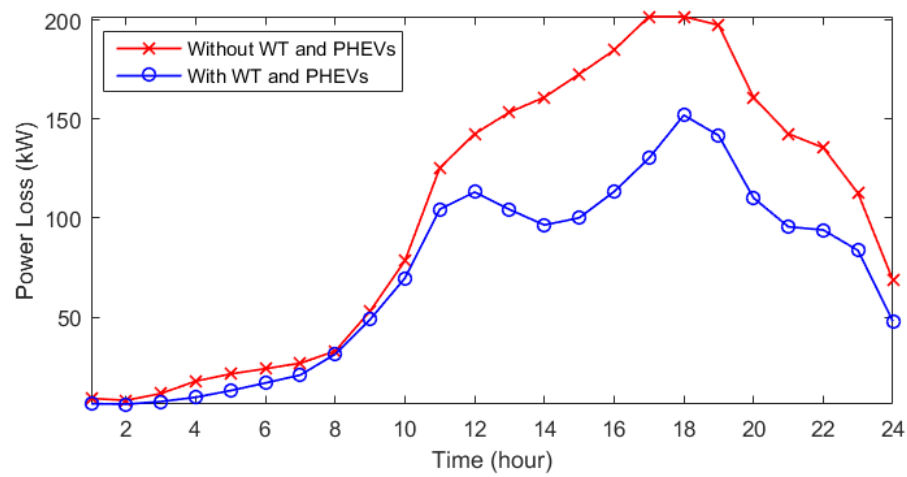


Figure 7. Power loss of the 33-bus distribution network with and without WT and PHEVs using the IGJO.

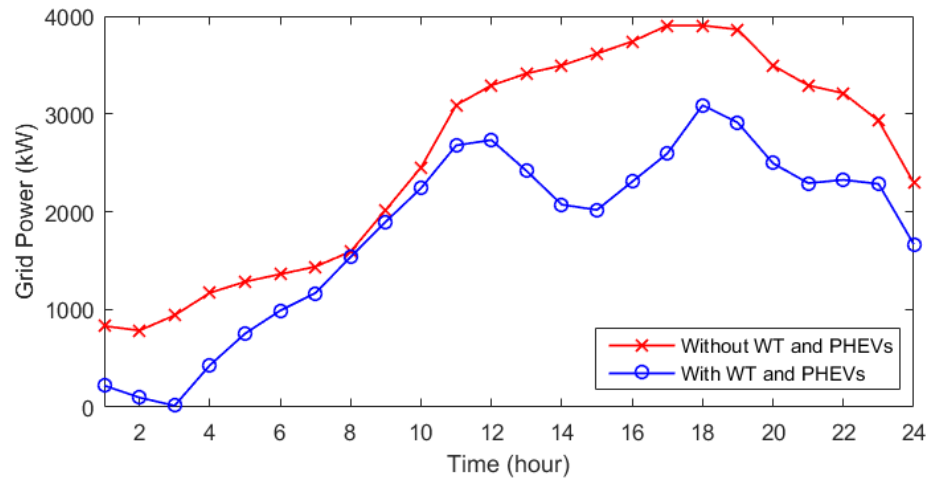


Figure 8. Received grid power with and without WT and PHEVs using the IGJO for 24 h.

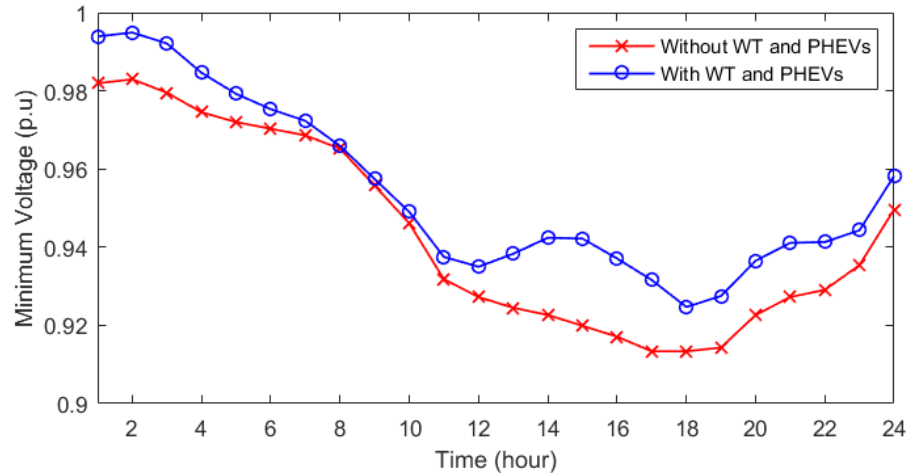


Figure 9. Minimum voltage of a 33-bus distribution network with and without WT and PHEVs using the IGJO for 24 h.

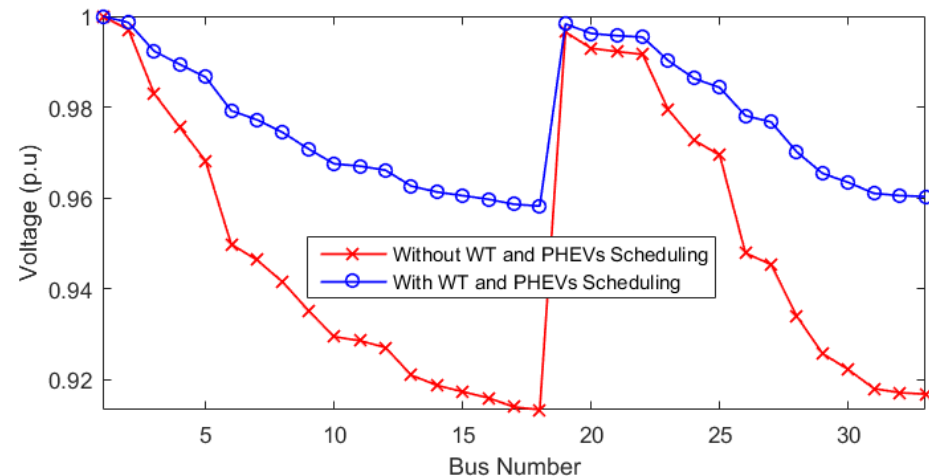


Figure 10. Voltage profile of a 33-bus distribution network with and without WT and PHEVs using the IGJO.

4.3. Results with Battery Degradation Cost

In this condition, based on the trial-and-error method, the weighted coefficients of the cost of losses and voltage deviations are equal to 0.2, and the other objective functions are

considered to be 0.15. In Figure 11, the convergence process of the WT allocation and PHEV scheduling in the distribution network considering battery degradation cost is depicted, and it can be seen that the optimal solution has been achieved with a high convergence speed in iteration 28.

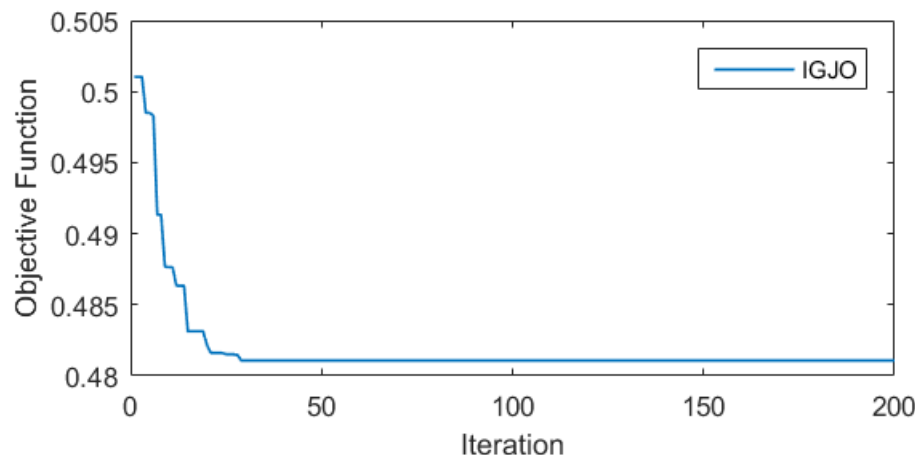


Figure 11. Convergence process of IGJO in allocation and scheduling of WT and PHEVs in the distribution network considering battery degradation cost.

The simulation results of the optimal solution and also the multi-objective allocation of WT and PHEV scheduling without and with consideration of battery degradation cost are presented and compared in Tables 6 and 7, respectively. Based on the results of the optimal solution in Table 6, it can be seen that in the case of not considering the cost of battery degradation, the optimization program has installed more wind power in bus 6 of the network. On the other hand, the optimization program has determined an amount of 764 kWh of the power capacity of the parking lots when considering the cost of battery degradation and 668 kWh when not including the cost of battery degradation. Therefore, taking into account the cost of battery degradation has increased the cost of parking lots and energy sources while reducing power loss and the cost of buying one from the main network. Additionally, the results have shown an improvement in the network voltage profile, considering the cost of battery degradation.

Table 6. The optimal solution without and with battery degradation cost.

Item/Algorithm	Without Degradation Cost	With Degradation Cost
WT location @bus/ peak size (kW)	@6/2941	@6/3000
PHEV location @bus/size	@7/80, @14/404, @21/41, @24/96, @29/47	@14/441, @32/323,

Taking into account the cost of battery degradation, the values of power loss cost, network energy cost, and network voltage deviations have been reduced by 3.28%, 1.07%, and 4.32%, respectively, compared to the case without battery wear degradation.

Figure 12 shows the power changes of the wind source over 24 h. In addition, the curve of changes in power losses and power purchased from the main network during 24 h is shown in Figures 13 and 14. It can be seen that by considering the cost of battery wear as a part of the objective function of the problem, it has reduced the power loss as well as the power purchased from the main grid at different hours.

Table 7. The results of WT and PHEV scheduling in the distribution network without and with battery degradation cost.

Item/Algorithm	Base Network	Without Degradation Cost	With Degradation Cost
Cost of energy losses (\$)	53,531	37,596	35,840
Reduction in C_{ELoss} (%)	–	29.76	33.04
Cost of grid energy (\$)	4,482,550	1,530,300	1,482,307
Reduction in C_{EGrid} (%)	–	65.86	66.93
Voltage deviation (p.u.)	0.0173	0.0140	0.0133
Reduction in VD (%)	–	18.80	23.12
Cost of PHEVs (\$)	–	620,356	635,739
Cost of WT (\$)	–	959,070	1,032,572
Cost of battery degradation (\$)	–	–	9607
OF	–	0.62577	0.4811

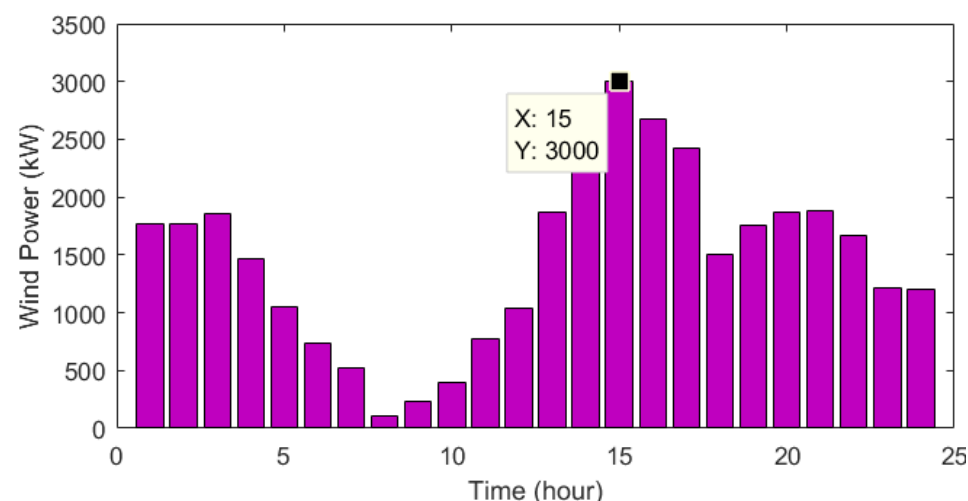


Figure 12. Wind power using the IGJO during 24 h with battery degradation cost.

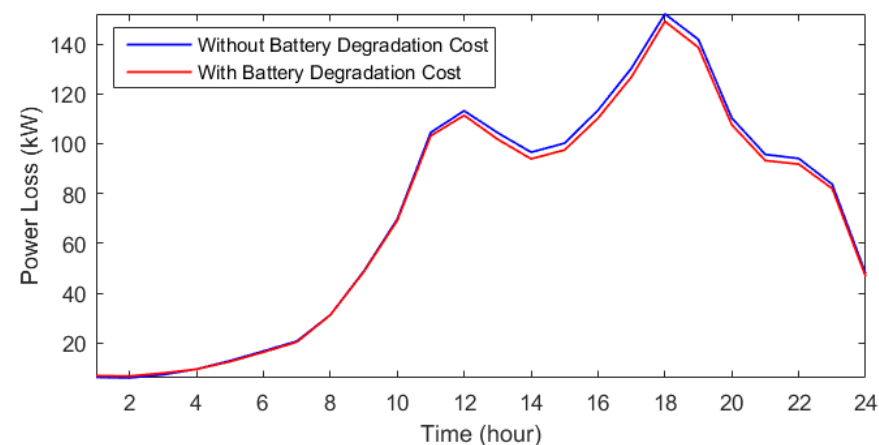


Figure 13. Power loss of the 33-bus distribution network without and with battery degradation cost using the IGJO.

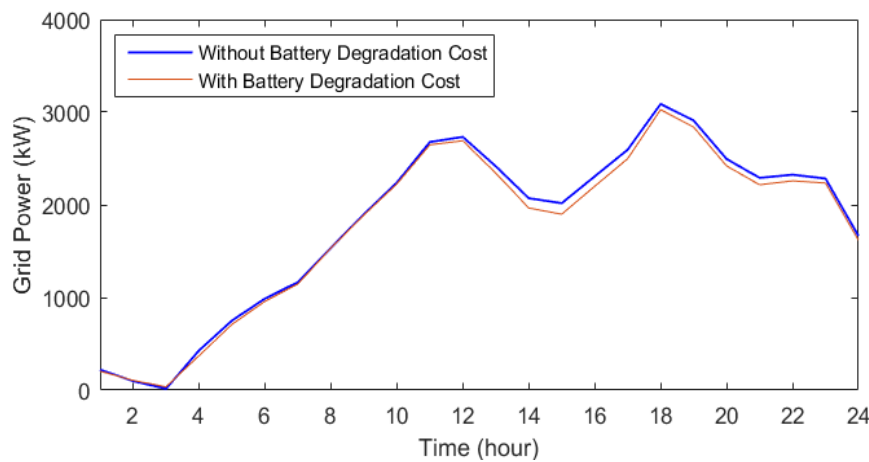


Figure 14. Received grid power without and with battery degradation costs using the IGJO.

The curve of minimum network voltage changes during 24 h as well as the network voltage profile are presented in Figures 15 and 16, respectively. The results show that by considering the cost of battery degradation, the voltage conditions have improved and the amount of voltage deviations compared to the state without considering the cost of battery degradation is reduced.

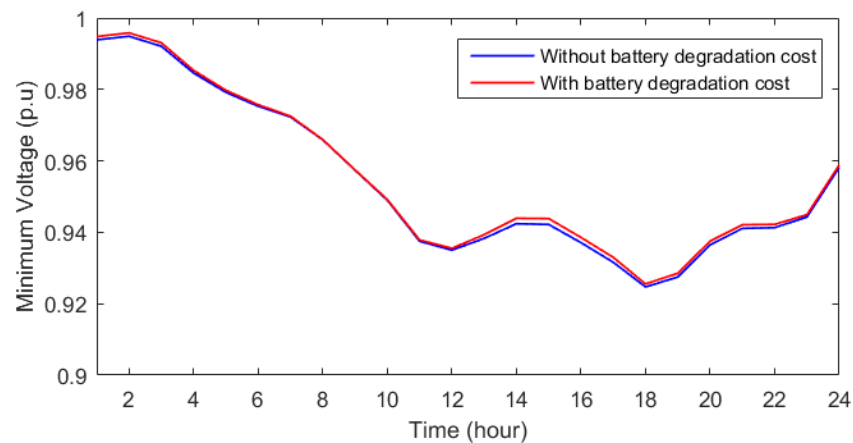


Figure 15. Minimum voltage of the 33-bus distribution network without and with battery degradation cost using the IGJO during 24 h.

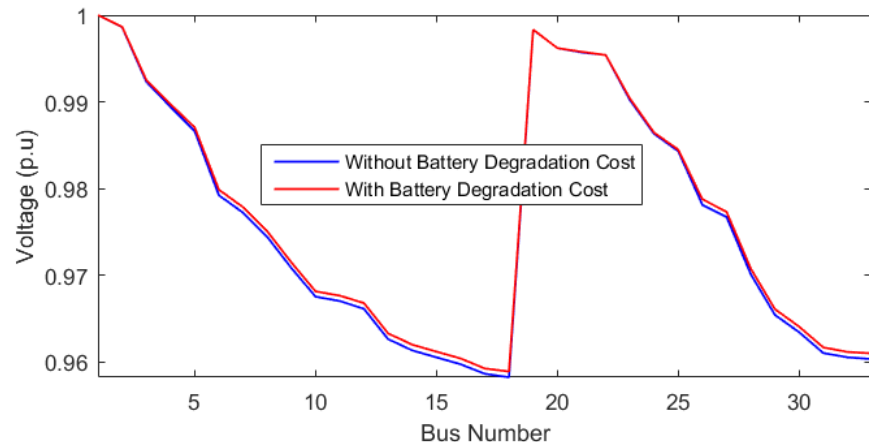


Figure 16. Voltage profile of the 33-bus distribution network without and with battery degradation costs using the IGJO.

4.4. The impact of PHEVs' Availability

In the last section, the reports on simulating the multi-objective siting and scheduling of wind turbines and electric parking lots in the distribution network, considering 100% availability for installed vehicles using the IGJO algorithm, are given. In this section, the results of considering different availability levels of electric vehicles from 100% to 10% in solving the problem of the imposed cost of power loss, upstream grid energy, and network voltage variations are presented according to Table 8. As is observed, the cost of power loss per year, the cost of upstream grid energy per year, and network voltage deviations have increased (decreased) with the decrease (increase) in the availability of vehicles. For example, for availability of 100%, 50%, and 10%, the cost of energy losses is obtained at USD 37,596, USD 46,044, and USD 49,603, respectively; the cost of main grid energy is achieved at USD 1,530,300, USD 1,911,643, and USD 2,106,993, respectively; and the network voltage deviations are obtained at 0.0140 p.u., 0.0161 p.u., and 0.0172 p.u., respectively.

Table 8. The impact of PHEVs' availability on costs of losses, grid energy, and voltage deviation.

Availability	Item/Algorithm	IGJO
100%	Cost of Power Loss (\$)	37,596
	Cost of Grid Energy (\$)	1,530,300
	Voltage deviation (p.u.)	0.0140
90%	Cost of power loss (\$)	38,895
	Cost of grid energy (\$)	1,668,950
	Voltage deviation (p.u.)	0.0142
80%	Cost of power loss (\$)	39,314
	Cost of grid energy (\$)	1,722,149
	Voltage deviation (p.u.)	0.0144
70%	Cost of power loss (\$)	42,465
	Cost of grid energy (\$)	1,817,067
	Voltage deviation (p.u.)	0.0148
60%	Cost of power loss (\$)	44,576
	Cost of grid energy (\$)	1,853,514
	Voltage deviation (p.u.)	0.0155
50%	Cost of power loss (\$)	46,044
	Cost of grid energy (\$)	1,911,643
	Voltage deviation (p.u.)	0.0161
40%	Cost of power loss (\$)	47,196
	Cost of grid energy (\$)	1,945,643
	Voltage deviation (p.u.)	0.0162
30%	Cost of power loss (\$)	47,892
	Cost of grid energy (\$)	2,004,643
	Voltage deviation (p.u.)	0.0165
20%	Cost of power loss (\$)	48,734
	Cost of grid energy (\$)	2,067,610
	Voltage deviation (p.u.)	0.0167
10%	Cost of power loss (\$)	49,603
	Cost of grid energy (\$)	2,106,993
	Voltage deviation (p.u.)	0.0172

4.5. Comparison with Previous Studies

In this section, the performance of the proposed method in wind resource allocation and scheduling the parking lots in the 33-bus distribution network using the IGJO is compared with that of ref. [36]. In [36], the optimal planning of parking lots and capacitors is performed using the quantum-behaved and Gaussian dragonfly algorithm (QGDA). The performance of the proposed method is compared with ref. [36] using the QGDA, PSO, and BBO in achieving the highest percentage of power loss reduction in the distribution network in Table 9. The results showed that the proposed methodology of planning electric parking lots and allocating wind resources in the network had achieved a higher percentage reduction in power losses than the QGDA, PSO, and BBO. Therefore, the

proposed methodology-based IGJO has shown better performance in reducing network power losses.

Table 9. Comparison of proposed methodology with previous studies.

Item/Algorithm	IGJO	QGDA1 [36]	QGDA2 [36]	BBO2 [36]	PSO2 [36]
Reduction in energy losses (%)	33.04	25.61	31.09	29.47	15.59

QGDA1: Only PHEVs, QGDA2: PHEVs + Capacitor, BBO2 and PSO2: PHEVs + Capacitor.

5. Conclusions

The present study addressed the optimal multi-objective siting and scheduling of wind turbines and electric parking lots in the 33-bus distribution system to minimize the costs imposed by power loss, main grid energy, wind energy, battery degradation, and PHEVs during a year, in addition to network voltage profile enhancement using IGJO's improved meta-heuristic method based on Rosenbrock's direct rotational strategy. The optimal places and scales of the wind turbines and EV parking lots were determined based on the IGJO. The simulation results showed that the methodology relying on the IGJO was able to find the optimal solution with the best statistical evaluation criteria and also the greatest improvement in various objectives compared to the traditional GJO, AEFA, PSO, and MRFO algorithms. The proposed methodology based on the IGJO has reduced the costs of energy losses and purchased energy from the power system and the voltage deviations of the 33-bus network compared to the basic state of the network by 29.76%, 65.86%, and 18.80%, respectively, which indicates its superior performance was confirmed in comparison to other methods. Moreover, considering the battery degradation cost, the energy losses cost, the grid energy cost, and voltage deviations of the distribution network are decreased by 3.28%, 1.07%, and 4.32%, respectively, in comparison to the case without battery degradation. The results showed that with the reduction (increase) in car availability in parking lots, the cost of energy losses and network energy increased (decreased), and the network voltage profile was also weakened (strengthened). By changing the availability from 100% to 10%, the cost resulting from power loss, the cost due to upstream grid energy, and network voltage deviations have increased by 31.94%, 37.68%, and 22.86%, respectively. Allocation and multi-objective scheduling of wind turbines and electric parking lots in an unbalanced distribution network to improve power quality indices are suggested for future work.

Author Contributions: J.Y. and J.X. were responsible for investigating the concepts and reviewing the systems and methods. They also contributed to the survey studies and methods and originated the presented ideas, while collaborating with P.L.Y., C.S.K. and Y.-L.C. on the manuscript. These individuals provided valuable suggestions regarding the experimental setup and analytical results. J.X., Y.-L.C. and P.L.Y. also contributed to the research ideas and analytical results and helped write the manuscript. Funding support was generously provided by Y.-L.C., who also co-wrote the manuscript with the rest of the team. M.B. contributed to the implementation of the mathematical optimization algorithm and to the statistical analysis. All authors have read and agreed to the published version of the manuscript.

Funding: This work was also funded by the National Science and Technology Council in Taiwan, under grant numbers NSTC-109-2628-E-027-004-MY3, NSTC-111-2218-E-027-003, and NSTC-111-2622-8-027-009, and also supported by the Ministry of Education of Taiwan under Official Document No. 1112303249 entitled "The study of artificial intelligence and advanced semi-conductor manufacturing for female STEM talent education and industry–university value-added cooperation pro-motion".

Institutional Review Board Statement: Not applicable.

Informed Consent Statement: Not applicable.

Data Availability Statement: Not applicable.

Conflicts of Interest: The authors declare no conflict of interest.

References

- Haji-Aghajani, E.; Hasanzadeh, S.; Heydarian-Foroushani, E. A novel framework for planning of EV parking lots in distribution networks with high PV penetration. *Electr. Power Syst. Res.* **2023**, *217*, 109156. [\[CrossRef\]](#)
- Naderipour, A.; Abdul-Malek, Z.; Arabi Nowdeh, S.; Gandoman, F.H.; Hadidian Moghaddam, M.J. A multi-objective optimization problem for optimal site selection of wind turbines for reduce losses and improve voltage profile of distribution grids. *Energies* **2019**, *12*, 2621. [\[CrossRef\]](#)
- Pirouzi, A.; Aghaei, J.; Pirouzi, S.; Vahidinasab, V.; Jordehi, A.R. Exploring potential storage-based flexibility gains of electric vehicles in smart distribution grids. *J. Energy Storage* **2022**, *52*, 105056. [\[CrossRef\]](#)
- Norouzi, M.; Aghaei, J.; Pirouzi, S.; Niknam, T.; Fotuhi-Firuzabad, M. Flexibility pricing of integrated unit of electric spring and EVs parking in microgrids. *Energy* **2022**, *239*, 122080. [\[CrossRef\]](#)
- Mojarad, M.; Sedighizadeh, M.; Dosaranian-Moghadam, M. Optimal allocation of intelligent parking lots in distribution system: A robust two-stage optimization model. *IET Electr. Syst. Transp.* **2022**, *12*, 102–127. [\[CrossRef\]](#)
- Naderipour, A.; Kamyab, H.; Klemeš, J.J.; Ebrahimi, R.; Chelliapan, S.; Nowdeh, S.A.; Abdullah, A.; Marzbali, M.H. Optimal design of hybrid grid-connected photovoltaic/wind/battery sustainable energy system improving reliability, cost and emission. *Energy* **2022**, *257*, 124679. [\[CrossRef\]](#)
- Alanazi, A.; Alanazi, M.; Nowdeh, S.A.; Abdelaziz, A.Y.; El-Shahat, A. An optimal sizing framework for autonomous photovoltaic/hydrokinetic/hydrogen energy system considering cost, reliability and forced outage rate using horse herd optimization. *Energy Rep.* **2022**, *8*, 7154–7175. [\[CrossRef\]](#)
- Hafez, O.; Bhattacharya, K. Optimal design of electric vehicle charging stations considering various energy resources. *Renew. Energy* **2017**, *107*, 576–589. [\[CrossRef\]](#)
- Moradijooz, M.; Moghaddam, M.P.; Haghifam, M.R.; Alishahi, E. A multi-objective optimization problem for allocating parking lots in a distribution network. *Int. J. Electr. Power Energy Syst.* **2013**, *46*, 115–122. [\[CrossRef\]](#)
- Arias, N.B.; Franco, J.F.; Lavorato, M.; Romero, R. Metaheuristic optimization algorithms for the optimal coordination of plug-in electric vehicle charging in distribution systems with distributed generation. *Electr. Power Syst. Res.* **2017**, *142*, 351–361. [\[CrossRef\]](#)
- Neyestani, N.; Damavandi, M.Y.; Shafie-Khah, M.; Contreras, J.; Catalão, J.P. Allocation of plug-in vehicles' parking lots in distribution systems considering network-constrained objectives. *IEEE Trans. Power Syst.* **2014**, *30*, 2643–2656. [\[CrossRef\]](#)
- Pahlavanhoseini, A.; Sepasian, M.S. Optimal planning of PEV fast charging stations using nash bargaining theory. *J. Energy Storage* **2019**, *25*, 100831. [\[CrossRef\]](#)
- Awasthi, A.; Venkitusamy, K.; Padmanaban, S.; Selvamuthukumaran, R.; Blaabjerg, F.; Singh, A.K. Optimal planning of electric vehicle charging station at the distribution system using hybrid optimization algorithm. *Energy* **2017**, *133*, 70–78. [\[CrossRef\]](#)
- Tabatabaee, S.; Mortazavi, S.S.; Niknam, T. Stochastic scheduling of local distribution systems considering high penetration of plug-in electric vehicles and renewable energy sources. *Energy* **2017**, *121*, 480–490. [\[CrossRef\]](#)
- El-Bayeh, C.Z.; Zellagui, M.; Shirzadi, N.; Eicker, U. A novel optimization algorithm for solar panels selection towards a self-powered EV parking lot and its impact on the distribution system. *Energies* **2021**, *14*, 4515. [\[CrossRef\]](#)
- Ahmadi, M.; Hosseini, S.H.; Farsadi, M. Optimal allocation of electric vehicles parking lots and optimal charging and discharging scheduling using hybrid metaheuristic algorithms. *J. Electr. Eng. Technol.* **2021**, *16*, 759–770. [\[CrossRef\]](#)
- Mirzaei, M.J.; Kazemi, A. A two-step approach to optimal management of electric vehicle parking lots. *Sustain. Energy Technol. Assess.* **2021**, *46*, 101258. [\[CrossRef\]](#)
- Mirzaei, M.J.; Siano, P. Dynamic long-term expansion planning of electric vehicle parking lots considering lost opportunity cost and energy saving. *Int. J. Electr. Power Energy Syst.* **2022**, *140*, 108066. [\[CrossRef\]](#)
- Wu, H.; Pang, G.K.H.; Choy, K.L.; Lam, H.Y. Dynamic resource allocation for parking lot electric vehicle recharging using heuristic fuzzy particle swarm optimization algorithm. *Appl. Soft Comput.* **2018**, *71*, 538–552. [\[CrossRef\]](#)
- Sattarpour, T.; Farsadi, M. Parking lot allocation with maximum economic benefit in a distribution network. *Int. Trans. Electr. Energy Syst.* **2017**, *27*, e2234. [\[CrossRef\]](#)
- Bilal, M.; Rizwan, M. A meta-heuristic-based optimal placement of distributed generation sources integrated with electric vehicle parking lot in distribution network. In *Smart Grids for Renewable Energy Systems, Electric Vehicles and Energy Storage Systems*; CRC Press: Boca Raton, FL, USA, 2022; pp. 167–190.
- El-Zonkoly, A.; dos Santos Coelho, L. Optimal allocation, sizing of PHEV parking lots in distribution system. *Int. J. Electr. Power Energy Syst.* **2015**, *67*, 472–477. [\[CrossRef\]](#)
- Das, S.; Thakur, P.; Singh, A.K.; Singh, S.N. Optimal management of vehicle-to-grid and grid-to-vehicle strategies for load profile improvement in distribution system. *J. Energy Storage* **2022**, *49*, 104068. [\[CrossRef\]](#)
- Chopra, N.; Ansari, M.M. Golden jackal optimization: A novel nature-inspired optimizer for engineering applications. *Expert Syst. Appl.* **2022**, *198*, 116924. [\[CrossRef\]](#)
- Rosenbrock, H. An automatic method for finding the greatest or least value of a function. *Comput. J.* **1960**, *3*, 175–184. [\[CrossRef\]](#)
- Abualigah, L.; Diabat, A.; Zitar, R.A. Orthogonal Learning Rosenbrock's Direct Rotation with the Gazelle Optimization Algorithm for Global Optimization. *Mathematics* **2022**, *10*, 4509. [\[CrossRef\]](#)

27. Moghaddam MJ, H.; Kalam, A.; Nowdeh, S.A.; Ahmadi, A.; Babanezhad, M.; Saha, S. Optimal sizing and energy management of stand-alone hybrid photovoltaic/wind system based on hydrogen storage considering LOEE and LOLE reliability indices using flower pollination algorithm. *Renew. Energy* **2019**, *135*, 1412–1434. [[CrossRef](#)]
28. Hadidian-Moghaddam, M.J.; Arabi-Nowdeh, S.; Bigdeli, M.; Azizian, D. A multi-objective optimal sizing and siting of distributed generation using ant lion optimization technique. *Ain Shams Eng. J.* **2018**, *9*, 2101–2109. [[CrossRef](#)]
29. Jafar-Nowdeh, A.; Babanezhad, M.; Arabi-Nowdeh, S.; Naderipour, A.; Kamyab, H.; Abdul-Malek, Z.; Ramachandaramurthy, V.K. Meta-heuristic matrix moth-flame algorithm for optimal reconfiguration of distribution networks and placement of solar and wind renewable sources considering reliability. *Environ. Technol. Innov.* **2020**, *20*, 101118. [[CrossRef](#)]
30. Naderipour, A.; Nowdeh, S.A.; Saftjani, P.B.; Abdul-Malek, Z.; Mustafa MW, B.; Kamyab, H.; Davoudkhani, I.F. Deterministic and probabilistic multi-objective placement and sizing of wind renewable energy sources using improved spotted hyena optimizer. *J. Clean. Prod.* **2021**, *286*, 124941. [[CrossRef](#)]
31. Sun, H.; Ebadi, A.G.; Toughani, M.; Nowdeh, S.A.; Naderipour, A.; Abdulla, A. Designing framework of hybrid photovoltaic-biowaste energy system with hydrogen storage considering economic and technical indices using whale optimization algorithm. *Energy* **2022**, *238*, 121555. [[CrossRef](#)]
32. Arabi-Nowdeh, S.; Nasri, S.; Saftjani, P.B.; Naderipour, A.; Abdul-Malek, Z.; Kamyab, H.; Jafar-Nowdeh, A. Multi-criteria optimal design of hybrid clean energy system with battery storage considering off-and on-grid application. *J. Clean. Prod.* **2021**, *290*, 125808. [[CrossRef](#)]
33. Alanazi, A.; Alanazi, M.; Nowdeh, S.A.; Abdelaziz, A.Y.; Abu-Siada, A. Stochastic-Metaheuristic Model for Multi-Criteria Allocation of Wind Energy Resources in Distribution Network Using Improved Equilibrium Optimization Algorithm. *Electronics* **2022**, *11*, 3285. [[CrossRef](#)]
34. Lotfipour, A.; Afrakhte, H. A discrete Teaching–Learning-Based Optimization algorithm to solve distribution system reconfiguration in presence of distributed generation. *Int. J. Electr. Power Energy Syst.* **2016**, *82*, 264–273. [[CrossRef](#)]
35. Javidsharifi, M.; Niknam, T.; Aghaei, J.; Mokryani, G. Multi-objective short-term scheduling of a renewable-based microgrid in the presence of tidal resources and storage devices. *Appl. Energy* **2018**, *216*, 367–381. [[CrossRef](#)]
36. Rajesh, P.; Shajin, F.H. Optimal allocation of EV charging spots and capacitors in distribution network improving voltage and power loss by Quantum-Behaved and Gaussian Mutational Dragonfly Algorithm (QGDA). *Electr. Power Syst. Res.* **2021**, *194*, 107049. [[CrossRef](#)]

Disclaimer/Publisher’s Note: The statements, opinions and data contained in all publications are solely those of the individual author(s) and contributor(s) and not of MDPI and/or the editor(s). MDPI and/or the editor(s) disclaim responsibility for any injury to people or property resulting from any ideas, methods, instructions or products referred to in the content.